ACS APPLIED BIO MATERIALS

www.acsabm.org

Forum Article

A Tunable Tumor Microenvironment through Recombinant Bacterial Collagen-Hyaluronic Acid Hydrogels

Stephanie Nemec, Sylvia Ganda, Karrar Al Taief, Chantal Kopecky, Rhiannon Kuchel, Hélène Lebhar, Christopher P. Marquis, Pall Thordarson, and Kristopher A. Kilian*

Cite This: https://doi.org/10.1021/acsabm.2c00186

Read Online

ACCESS | Metrics & More | Article Recommendations | Supporting Information

ABSTRACT: Laboratory models of the tumor microenvironment require control of mechanical and biochemical properties to ensure accurate mimicry of patient disease. In contrast to pure natural or synthetic materials, hybrid approaches that pair recombinant protein fragments with synthetic scaffolding show many advantages. Here we demonstrate production of a recombinant bacterial collagen-like protein (CLP) for thiol−ene pairing to norbornene functionalized hyaluronic acid (NorHA). The resultant hydrogel material shows an adjustable modulus with evidence for strain-stiffening behavior that resembles natural tumor matrices. Cysteine terminated peptide binding motifs are incorporated to adjust the cell-adhesion points. The modular hybrid gel shows good biocompatibility and was demonstrated to control cell adhesion, proliferation, and the invasive properties of MCF7 and MD-MBA-231 breast adenocarcinoma cells. The ease in which multiple structural and bioactive components can be integrated provides a robust framework to form models of the tumor microenvironment for fundamental studies and drug development.

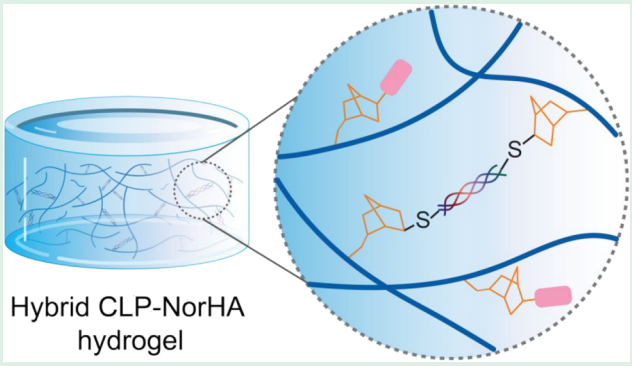

KEYWORDS: *tumor microenvironment, bacterial collagen, hyaluronic acid, hydrogel, extracellular matrix*

INTRODUCTION

Synthetic peptide-based materials used to create hydrogels enable a blank-slate, tunable platform for mimicking the tumor microenvironment (TME). However, synthetic materials often lack the rich structural and biochemical complexity inherent to natural hydrogels. Recombinant DNA approaches have served as a middle ground, providing a route to reproducibly generate pieces of complex matrices, such as coiled coils[1,2] and collagen triple helices,[3] that can be tagged for linking within synthetic scaffolding.[4] Uniquely, synthetic materials facilitate the decoupling of mechanical properties from biological motifs, where both can be varied independently to optimize cellular processes. By creating these hybrid natural-synthetic hydrogels, diverse biomaterials with modular components can be integrated to mimic aspects of a native TME. In this way, complex and diverse cell−TME interactions can be modeled *in vitro* using dispersed single cells, densely packed spheroids, or heterotypic combinations.

While there have been considerable advances in hybrid hydrogel systems and synthetic mimics,[5,6] the biomaterials community has yet to advance a reliable and reproducible system to challenge biological gold-standard materials such as collagen and Matrigel. Matrigel, GelTrex, and other Engelbreth-Holm-Swarm-derived hydrogel substrates contain basement membrane proteins, primarily laminin, collagen IV, heparan sulfate proteoglycans, entactin/nidogen, and other growth factors. These natural ECM products have batch-to-batch variability, making them unsuitable for reproducible *in vitro* studies.[5] Nevertheless, these natural-derived materials remain the optimal choice for mimicking the ECM of fibrous, stroma-enriched tumors such as breast, prostate, and pancreatic cancers. These cancers share similarities in the TME, with a diverse network of proteins and proteoglycans including fibrillar collagens, laminins, fibronectin, proteoglycans, and hyaluronic acid.[7]

As an alternative to reconstituted tissue, recombinant approaches to generate natural matrices have had some success, including the generation of fibrillar collagen.[8] Various recombinant proteins such as elastin and laminin have been leveraged to generate advanced tissue and disease models with tunable mechanical and biological properties.[9−11] However, the reproducible generation of biomimetic structural human collagen for wide-scale use remains a challenge. Recombinant

Special Issue: Self-Assembling Biomaterials from Proteins, Peptides, and DNA

Received: February 28, 2022
Accepted: May 22, 2022

collagen-like proteins (CLP) have been expressed in *Escherichia coli* (*E. coli*) for applications ranging from cosmetics to tissue engineering.[12,13] These bacterial CLPs display thermal stability with the *Streptococcal pyogen* (*S. pyogen*) Scl2 protein generating a triple-helix one-fifth the length of fibrillar mammalian collagen and notably biologically inert or "blank slate".[13] In this way, Scl2 protein can be leveraged in biomaterial models of collagen function. Cosgriff-Hernandez et al. demonstrated Scl2 protein triple helices in a hybrid gel with poly(ethylene glycol) diacrylate (PEGDA), and Parmar et al. followed with Scl2 containing hydrolytically or enzymatically cleavable matrix metalloproteinases (MMPs) and aggrecanases for applications in cartilage regeneration.[14−16]

In this study, we developed a hybrid hydrogel system comprised of recombinant collagen-like protein (CLP) and functionalized hyaluronic acid (HA). HA is a ubiquitous ECM component ranging from short oligosaccharides (5−40 kDa) to 100 kDa in serum and 8 MDa in the vitreous.[17,18] The HA backbone can be functionalized with pendant cross-linkable groups such as methacrylate, aldehyde, and norbornene groups.[19,20] We developed a CLP containing two cysteines at the N-termini to form a hydrogel via thiol−ene coupling to a norbornene functionalized HA. The remaining unbound norbornene were reacted with a cysteine terminated cell-adhesive arginine-glycine-aspartate (RGD) peptide motif.[21] Shear rheology demonstrated tunable mechanical properties along with strain-stiffening behavior that resembles natural matrices. Cell−matrix interactions of CLP-HA hydrogels were investigated using nonmetastatic and metastatic breast cancer cells and spheroids, comparing RGD functionalized material with a scrambled, nonadhesive control arginine-aspartate-glycine (RDG). The modular combination of CLP, HA, and short peptides provides a biocompatible material, where growth and migration can be monitored as a model of the TME.

2. METHODS

2.1. Collagen-Like Protein Synthesis, Purification, and Characterization. *2.1.1. CLP Synthesis.* Recombinant *Streptococcal* collagen-like 2.28 (Scl2.28) protein was expressed in *Escherichia coli* BL21(DE3). The blank slate bacterial collagen-like protein construct was derived from the pD441-NH vector (ATUM) with an isopropyl *β*-D-1-thiogalactopyranoside (IPTG)-inducible, T5 promoter with a His tag, and kanamycin resistance. A shortened version of a pColdIII-163 polypeptide sequence (Parmar 2015) was used containing a globular domain (V), enzyme cleavage site (LVPRGSP), stabilizer (GGPCPPC), and collagen-like domains (ABC) and then another stabilizer. *E. coli* were grown in 2YT media with kanamycin (100 μg/mL) at 30 °C at 180 rpm overnight and then diluted into fresh media, incubated at 37 °C at 200 rpm, and the growth monitored until the OD600 reached 0.6 when 1 mM IPTG was added to induce protein expression for 3 h. Protein was extracted from bacterial pellets resuspended in 20 mM sodium phosphate buffer, 500 mM NaCl, and 20 mM imidazole and lysed by sonication for 8 min on ice 2 on 2 s off. Cell debris was pelleted by centrifugation at 10 000*g* for 30 min at 4 °C, and supernatant containing the CLP was retained.

2.1.2. CLP SDS-PAGE Expression Test. CLP expression and solubility was characterized by electrophoresis. Sodium dodecyl sulfate-polyacrylamide gel electrophoresis (SDS-PAGE) analysis was used to confirm induced, soluble protein. Denatured proteins were incubated at 95 °C for 5 min with 2% *β*-mercaptoethanol. Nondenatured samples were incubated in 5% glycerol and kept on ice prior to electrophoresis on 12% SDS-PAGE gels. Gels were stained with Coomassie blue, and protein migration was compared to molecular weight marker standards.

2.1.3. CLP Purification. The CLP was purified through acid extraction by adjusting the pH to 2.2 in 50 mM acetic acid at 4 °C for 16 h. The V domain was cleaved with 0.01 mg/mL pepsin at 4 °C for 16 h. The pH was adjusted back to 7 using NaOH to stop the reaction.[22] The CLP was further purified with a 30 kDa centrifugal filter (Amicon Ultra-15) according to manufacturer instructions. Purity was measured by SDS-PAGE (Figure S1).

2.1.4. CLP Secondary Structure. Circular dichroism (CD) spectra of purified CLP in H_2O was gathered on an Applied PhotoPhysics Chirascan Plus spectrometer controlled by Applied PhotoPhysics Pro-Data SX software equipped with a Peltier temperature control system using a 1 mm path length quartz cuvette (Starna Pty Ltd.). The spectra were monitored between 190 and 280 nm with step size and bandwidth 1 nm.

2.1.5. Transmission Electron Microscopy (TEM). The samples for electron microscopy were prepared by the drop casting method. Briefly, 5 μL of CLP solution was deposited onto a plasma-treated carbon-coated copper grid (square mesh 200, Ted Pella Australia). The droplet was left on the grid for 1 min and the excess liquid blotted off with a filter paper. The grid was dried by blowing a gentle stream of N_2 and left to air-dry overnight prior to analysis. Bright-field transmission electron microscopy (TEM) micrographs were obtained on FEI Tecnai G2 20 TEM operating at an accelerating voltage of 200 kV. Images were acquired using a Gatan Orius Camera. The TEM images obtained were unstained.

2.2. NorHA Synthesis and Characterization. *2.2.1. NorHA Synthesis.* The synthesis of norbornene functionalized HA was carried out in two steps following a literature procedure[23] with slight modification. In the first step, HA was converted to tetrabutylammonium salt (HA-TBA) so that it would be soluble in dimethyl sulfoxide (DMSO) for a coupling reaction. Briefly, sodium hyaluronate (Na-HA, Lifecore Biomedical, ∼40 kDa) was dissolved in Milli-Q water at a concentration of 20 mg/mL by vigorous stirring. Once dissolved, Dowex resin (50WX8, Sigma-Aldrich) was added to the HA solution at 3:1 w/w ratio and was left stirring for 2 h at room temperature. Following, the resin was filtered from the mixture by vacuum filtration through a nylon filter cloth with 25 μm mesh size. The filtrate was neutralized to pH ∼7.0 by dropwise addition of tetrabutylammonium hydroxide (TBA−OH) solution (prepared by diluting TBA−OH 40 wt % with water to TBA−OH/H_2O = 1:1 v/v ratio). The resulting solution was frozen with liquid nitrogen and lyophilized to yield a slightly pink solid and used in the next step. ^{1}H NMR (400.17 MHz, DMSO-d_6) confirmed the presence of TBA as indicated by the peaks at δ = 3.18, 1.58, 1.32, and 0.94 ppm (Figure S2A).

For modification with norbornene, HA-TBA was first dissolved in anhydrous DMSO at 2 wt %. Following, 5-norbornene-2-methylamine (5.16×10^{-4} mol, 25 equiv to HA-TBA) was added to the solution mixture under vigorous stirring. Next, PyBOP (6.20×10^{-4} mol, 30 equiv to HA-TBA) and DIPEA (6.20×10^{-4} mol, 30 equiv to HA-TBA) were added to the mixture. The mixture was left stirring at room temperature for 2 h and quenched with cold water. The solution was then transferred to a presoaked dialysis membrane (MWCO 10 kDa) and purified by dialysis against NaCl solution (5 g/L) for 3 days and then water for another 3 days. The dialysate was changed twice daily in both cases. The final product was recovered by lyophilization to yield colorless low density solid. ^{1}H NMR (400.17 MHz, DMSO-d_6) confirmed the presence of norbornene pendants (Figure S2B). Determination of the degree of substitution (DS) of norbornene was calculated using the peaks at δ = 6.28−5.85 ppm from the vinyl protons of norbornene and at δ = 4.03−3.2 ppm from the protons on the carbohydrate moieties of HA. The DS of norbornene on HA was calculated to be 25%.

2.2.2. Nuclear Magnetic Resonance (NMR). ^{1}H NMR spectra were recorded using a Bruker Avance III HD 400 equipped with 5 mm BBFO+ probe (^{1}H, 400.17 MHz). NMR spectra were processed using Bruker TOPSPIN 3.6.2 software. Generally, norbornene-modified hyaluronic acid (NorHA) samples were prepared by dissolving 5 mg of polymer in 700 mL of D_2O with addition of 10 mL of NaOD (4%). The addition of NaOD reduced the viscosity of

https://doi.org/10.1021/acsabm.2c00186
ACS Appl. Bio Mater. XXXX, XXX, XXX−XXX

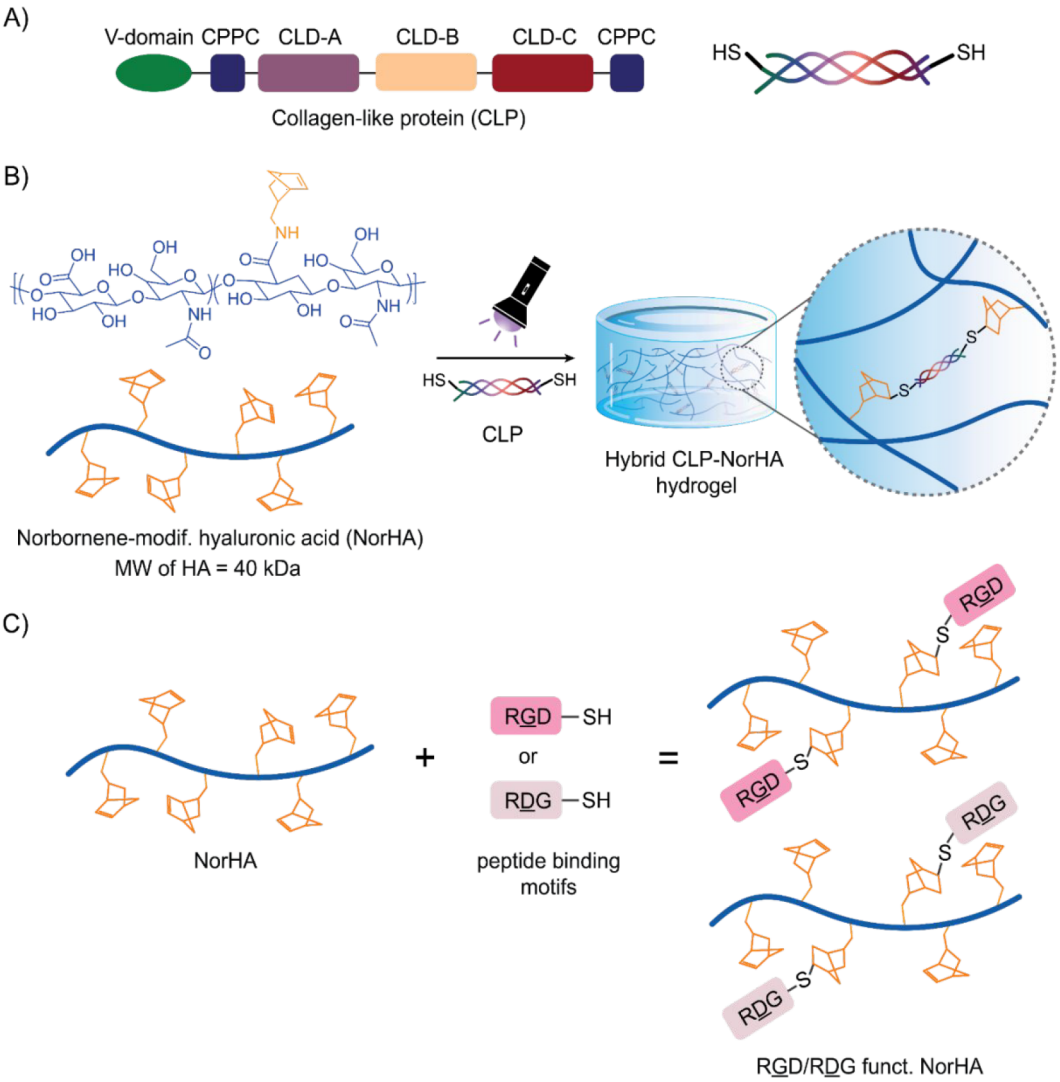

Figure 1. Schematic of recombinant hybrid collagen-like protein (CLP), norbornene functionalized hyaluronic acid hydrogel (NorHA). (A) Genetic construct of CLP containing a globular V-domain, two "CPPC" stabilizing sequences at both the N and C termini, and collagen-like domain (CLD) from *Scl2.28* protein comprised of three unique regions (A, B, C). (B) Norbornene functionalized (25%) hyaluronic acid backbone forms a hybrid CLP-NorHA hydrogel via light mediated cysteine-norbornene coupling. (C) Addition of integrin-binding GRGDSC (RGD) and scrambled GRDGSC (RDG) binding motifs to hybrid CLP-NorHA gels.

HA solution, allowing better resolution of the spectra collected. The spectra were acquired with 128 scans.

2.3. Preparation of Bioactive CLP-NorHA Hydrogels. *2.3.1. Hydrogel Cross-Linking.* To generate hydrogels, NorHA (25% norbornene) was weighed and sterilized with UV for 30 min. The NorHA was suspended to a final concentration of 1 or 2 wt % in complete medium (detailed in section 2.6.1) and vortexed until completely dissolved. CLP was added in a thiol/norbornene ratio of 1:1[20] with lithium phenyl-2,4,6-trimethylbenzoylphosphinate (LAP) at a final concentration of 0.5 wt %.

2.3.2. Scanning Electron Microscopy (SEM) Analysis. Collagen samples were fixed in 2.5% glutaraldehyde overnight at 4 °C. The samples were then rinsed twice in milli-Q water and dehydrated using an ethanol series (30%, 50%, 70%, 80%, 90%, 100%). The collagen was then processed using a Tousimis (Rockville, Maryland USA) critical point dryer. The dried samples were coated with a 10 nm thin layer of Pt (Leica EM ACE600, Wetzlar, Germany) and imaged using the FEI (Thermo Fisher) Nova NanoSEM 450 FE-SEM (Waltham, Massachusetts, USA) with an accelerating voltage of 5 keV and spot size 3.

2.4. Peptide. To promote cell adhesion, a thiol-containing, cell-adhesive GRGDSC (GenScript Biotech PTE LTD) oligopeptide was used. As a control. Scrambled nonadhesive GRDGSC (GenScript Biotech PTE Ltd.) was used. Briefly, GRGDSC or nonadhesive GRDGSC in water (1 mM) was added to the precursor solution to allow the peptides to react with the norbornene groups on the HA backbone via thiol−ene chemistry, initiated by LAP.

2.5. Rheology. *2.5.1. Rheological Time and Frequency Sweeps.* Rheological measurements were performed on Antor Paar MCR 302 rheometer fitted with a 25 mm diameter parallel plate and equipped with a Peltier-temperature-controlled hood (model H-PTD 200) and glass bottom plate. The distance gap was set to 1 mm, and all measurements were performed at 37 °C. A UV torch was placed beneath the glass plate for cross-linking of the hydrogel. For time sweep data, 600 μL of hydrogel were prepared and cast on the glass bottom plate. Time resolved rheology was applied with a constant 0.2% strain and 1 Hz frequency. Data points were collected every 6 s over 10 min measurements. Frequency sweeps were set to a logarithmic ramp starting from 10 to 0.1 Hz with constant 0.2% strain. Data points were collected every 2 s over 5 min. Measurements were repeated three times, and the average was plotted.

2.5.2. Rheological Strain Sweeps and Stiffening. Strain sweeps were set to a logarithmic ramp from 0.01% to 100% (low to high). Frequency was set to a constant 1 Hz with measurements taken every

https://doi.org/10.1021/acsabm.2c00186
ACS Appl. Bio Mater. XXXX, XXX, XXX−XXX

2 s for 5 min. For strain stiffening, a prestress protocol was adopted from Broedersz et al.[24] Briefly, measurement was set for 56 intervals. Each relaxation interval lasted for 180 s followed by a stress interval that was set for 150 s in each interval, and the oscillatory shear stress with constant frequency (τ) is set to be 1/10 of the shear stress. At each stress interval, shear stress was averaged and divided by 100. The differential modulus (K') was calculated as the average of shear stress divided by shear strain $K = \frac{\partial\sigma}{\partial\gamma}$ and plotted against stress (σ) (0.016−1009 Pa).

2.6. Cell Culture. *2.6.1. Human Breast Cancer Cell Lines.* Epithelial adenocarcinoma MCF7(ATCC) and MDA-MB-231 (ATCC) cells were used below passage 15. Both breast cancer cell lines were cultured with high glucose (4.5 g/L D-glucose) DMEM (Gibco, USA) with 10% fetal bovine serum (FBS) and passaged with 0.25% trypsin. Media was changed every 2 days, and cells were passaged at 80−90% confluency, 3 times per week for MCF7s, and 2 times per week for MDA-MB-231.

2.6.2. Spheroid Formation and Embedding. After lifting metastatic breast cancer cells from the tissue culture plastic flasks, cells were counted and 3 000 cells were added to each well of a 96-well round-bottom ultralow attachment microplate (Corning) and grown for 10 days. Media was removed such that 100 μL remained followed by transfer to the top of CLP-NorHA gels on glass-bottom 96-well plates (P96-0-N Cellvis) with an additional 200 μL of media. Brightfield images on an optical microscope (Ckx53SF Olympus, 4× objective) were captured using cellSens imaging software (Olympus) upon transfer (day 0) and days 5 and 7. For spheroid encapsulation, MCF-7 and MDA-MB-231 were seeded at 2000 cells and 4000 cells, respectively, in an ultralow attachment round-bottom 96 well microplate. At 72 h postformation, the media was carefully removed, the spheroids were embedded in the indicated CLP-NorHA gels (n = 4) and grown under normal culture conditions for an additional 6 days. Cell culture media was changed every 48 h, and brightfield images were taken every 48 h on an inverted light microscope (Olympus CKX53, 4× objective). Spheroid growth and outgrowth were quantified from brightfield images using a customized MATLAB script (MathWorks). Spheroid growth rate is shown as area % of day 0 (day of embedding). Spheroid outgrowth rate is shown as perimeter % of day 0 (day of embedding). Data are shown as means ± SD.

2.7. Biocompatibility Imaging. *2.7.1. Viability/Cytotoxicity Stain.* Media was removed off the top of samples. Calcein-AM and ethidium homodimer-1 (Invitrogen) were thawed and resuspended in PBS according to manufacturer instructions. The LIVE/DEAD dye mix was added to each respective well and incubated at 37 °C, 5% CO_2 for 30 min. The stain was removed and washed with PBS and a minimum incubation for 10 min two times. Samples were kept in PBS during imaging.

2.7.2. Light Scanning Confocal Microscopy. LSM 800 (Carl Zeiss, Germany) inverted Zeiss Axio Observer Z1 laser scanning confocal microscope with 10× (0.45 N.A., air, 2 mm working distance) objective lens was used for imaging.

3. RESULTS AND DISCUSSION

3.1. Characterization of Collagen-like Protein (CLP) and Norbornene Derivatized Hyaluronic Acid (NorHA). Recombinant *S. pyogen* collagen-like 2.28 (Scl2.28) protein with four domains, a globular V-domain at the N-terminus, a "CPPC" sequence for stabilizing and functionalizing through thiol−ene chemistry, three CL domains of 78−81 amino acids, and another "CPPC" at the C-terminus (Figure 1A), were expressed in *E. coli*.[13,25] A minimal synthetic CLP sequence was used to generate a triple-helical structure (Table S1). Gel electrophoresis confirmed induced, soluble expression of CLP (Figure 2A). Secondary structure analysis via circular dichroism of CLP showed a minimum at 205 nm and local maxima at 220 nm that after purification shifted to a higher magnitude minimum at 200 nm, closer to the 198 nm expected

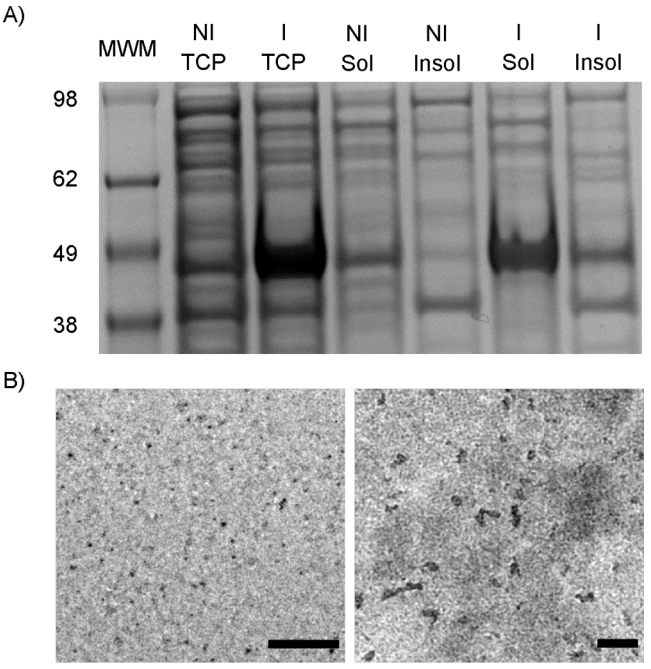

Figure 2. Characterization of collagen-like protein (CLP) via (A) electrophoresis CLP expression SDS-PAGE first lane, molecular weight marker (MWM); second lane, noninduced total cell protein (NI TCP); third lane, induced total cell protein (I TCP); fourth lane, noninduced soluble protein (NI Sol); fifth lane, noninduced insoluble protein (NI Insol); sixth lane, induced soluble protein (I Sol); seventh lane, induced insoluble protein (I Insol). (B) Transmission electron microscopy (TEM) images of collagen-like protein (CLP). Scale bars: 500 nm (left), 100 nm (right).

and 196 nm minima measured with bovine collagen (Figure S3). Further analysis via TEM revealed the generation of short, cylindrical-like nanostructures, confirming the successful preparation of short, collagen-like protein (CLP). The fragmented structures observed indicate the triple-helical folding of the collagen strands (Figure 2B). Next, 40 kDa hyaluronic acid was functionalized with norbornene (Figure 1B) which was confirmed with NMR (Figure S2). CLP and NorHA were combined in a 1:1 ratio of thiol/norbornene.[20] Cell-adhesive RGD and nonadhesive RDG binding motifs containing cysteine were added to decorate the NorHA backbone (Figure 1C).

3.2. Synthesis of CLP-NorHA Hybrid Hydrogel and Mechanical Properties. Recombinant CLP was produced in *E. coli* (~40 mg/L of 2YT) and scaled in a bioreactor to increase the yield for making hydrogels. The expressed protein was acid purified, concentrated, and maintained under reducing conditions (Figure S1). The UV-initiated thiol−norbornene chemistry used to cross-link (Figure S4) the materials was confirmed by an inversion test (Figure 3C). SEM imaging was used to assess structural characteristics of the material before and after cross-linking. Figure 3A shows SEM images of the unmodified CLP-NorHA which exhibits a dense network of short fibers tens of nanometers in length. Comparatively, after cross-linking, the material takes on a highly porous nanofibrous network with interconnected fibers of hundreds of nanometers. To understand the gelation kinetics, shear rheology was conducted during cross-linking of the hybrid CLP-NorHA hydrogel, demonstrating a liquid precursor with rapid gelation upon UV exposure, reaching a

https://doi.org/10.1021/acsabm.2c00186
ACS Appl. Bio Mater. XXXX, XXX, XXX−XXX

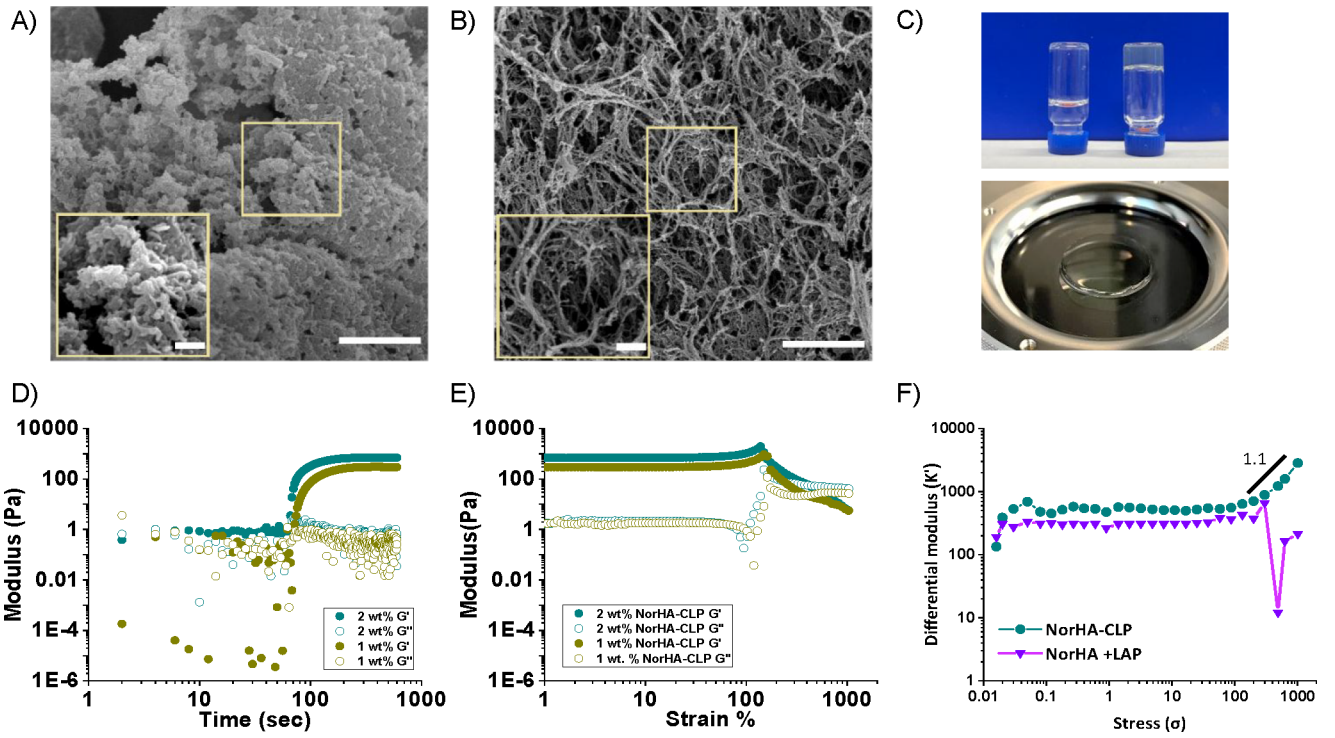

Figure 3. CLP-NorHA hydrogel synthesis. Scanning electron microscopy of (A) uncross-linked and (B) cross-linked samples. Scale bar 1 nm (inlay), 200 nm. (C) CLP-NorHA precursor (top-left) and gel (top-right) and photo-cross-linked on rheometer stage (bottom). (D) Time sweep rheology of CLP-NorHA gels containing 2 wt %, 1wt % NorHA with constant 1:1 norbornene/thiol precursor with UV light applied at 60 s to trigger gelation. (E) Strain sweep rheology of CLP-NorHA gels containing 2%, 1% NorHA with constant 1:1 norbornene/thiol gel. (F) Stiffening of 2 wt % NorHA-CLP (circle) and 2 wt % NorHA + LAP (triangle) hydrogel. Differential shear modulus K' vs shear stress σ for hydrogel at 37 °C. Hydrogels were cross-linked and plateaued via time-resolved rheology and then measured for strain stiffening.

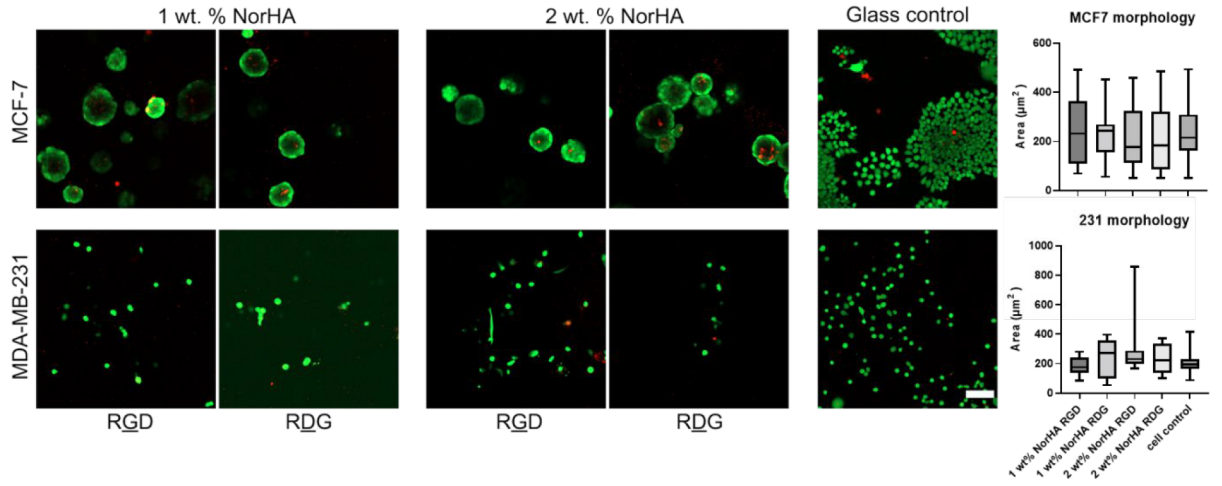

Figure 4. Biocompatibility of MCF7 and MDA-MB-231 cells after 4 days on top of 1 or 2 wt % NorHA-CLP gels containing RGD or RDG with a glass-bottom cell control (green-live; red-dead). Scale bar: 100 μm. Right: Quantification of cell area (μm^2) of MCF7 and MDA-MB-231 (231) cells.

stable storage modulus (700 Pa 2 wt % NorHA, 300 Pa 1 wt % NorHA) in less than 2 min (Figure 3D). The shear strain measurements show that both hydrogels do not deviate at 100% strain, the earliest sign of deviation from the linear viscoelastic region (LVR), a region where the hydrogel's modulus is plateaued and stabilized, is seen at 120% strain. Moreover, the modulus of both hydrogels has a steep incline at 139% stain for 2 wt % and 150% for 1 wt % hydrogel before the crossover point where the $G' = G''$, which is indicative of strain stiffening behavior of a hydrogel. Strain stiffening arises from strong cross-linking between HA and CLP, where elongation of the macromolecules resists strain at higher stress. This is similar to what is observed in native type I collagen.[26] In a relaxed state, the long chain of NorHA-CLP is not stretched, yet once stress is applied the cross-linked chain is stretched to its maximum. This behavior can also be seen in Figure 3E where more than 100% stain is needed to rupture the NorHA-CLP network. The hydrogel breaks at ~300% strain highlighting the additional stretching required to break the lengthened NorHA-CLP chain. Further strain stiffening

https://doi.org/10.1021/acsabm.2c00186
ACS Appl. Bio Mater. XXXX, XXX, XXX−XXX

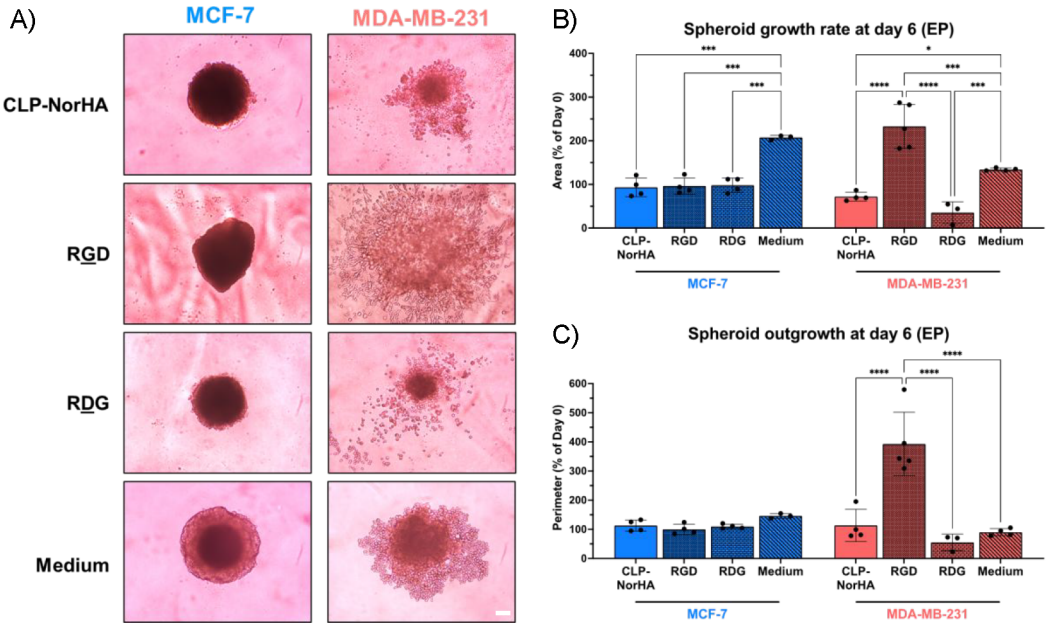

Figure 5. (A) Tumor spheroid encapsulation for MCF7 and MDA-MB-231 within 2 wt % NorHA-CLP gels containing RGD or RDG after 6 days of culture. Associated quantification of cell growth as determined by area (B) or outgrowth and matrix invasion as determined by change in perimeter (C). Scale bar: 100 μm.

indicates a backbone stretch with a slope of 1.1, indicating single filament stretching of hybrid CLP-NorHA gels demonstrating how the hybrid gel shows natural shear thickening properties, in strong contrast to the NorHA control (Figure 3F).[27]

3.3. Breast Cancer Viability on CLP-NorHA Hybrid Hydrogels. The CLP-NorHA hybrid gel system can be tuned to integrate any motif containing an accessible cysteine. For this study, we used a cell-binding RGD sequence (GRGDSC) and scrambled, noncell binding RDG motifs (GRDGSC; Figure 1C). Future work may include additional peptide motifs to tune peptide density and composition to suit the application. CLP-NorHA hybrid hydrogels can be tuned mechanically and biologically to represent a range of cancer environments including recreating aspects of the dense, ECM-rich breast cancer TME. Two metastatic breast cancer lines of varying invasive potential, MCF7 and MDA-MB-231, were tested in the hybrid gel system. Human breast cancer (MCF7, 231s) was added on top of CLP-NorHA gels containing 1 or 2 wt % NorHA with a constant 1:1 thiol/norbornene ratio with RGD or RDG peptide binding motif (1 mM). Cell viability was found to be ≥90% after culturing for 4 days using live/dead staining and laser scanning confocal microscopy (Figure 4). Importantly, 231 cells showed significantly more spreading and elongation on the CLP-NorHA gels containing RGD with some influence in spreading on account of stiffness with constant CLP content (thiol/norbornene ratio). Both breast cancer lines maintained high viability regardless of binding motif, indicating the good biocompatibility of the CLP-NorHA hybrid gels (Figure S5).

3.4. Comparing Invasive Spreading of Cancer Cells in CLP-NorHA. To more closely model a growing tumor, spheroids were generated on nonadherent plates for a tumor spheroid-based migration assay[28] and placed on gelled CLP-NorHA to observe the interface between the cancer mass and ECM. Aligned with the biocompatibility assay, spheroids of both MCF7 and 231s continued to grow on the hybrid gel (Figure S6). Next, we formed spheroids and encapsulated them within the CLP-NorHA material. There were very little differences between conditions for the MCF7 cells, consistent with previous studies that demonstrate these cells prefer to adhere to each other forming spheroids. The MCF7 spheroids had a visually dark, dense core with diminished growth when encapsulated in all hydrogel materials (Figure 5). In contrast, the 231 spheroids were smaller in size and loosely packed. We monitored the growth of the spheroids over time and observed striking differences for cells within the RGD modified material (Figures S7 and S8). By day 6, the embedded 231 spheroids showed evidence of increased cell spreading and invasive characteristics in the RGD functionalized CLP-NorHA, compared to spheroids on the scrambled RDG functionalized CLP-NorHA. We observed a pronounced difference in cell growth within the aggregate (Figure 5B) and outgrowth into the surrounding matrix when the material presented the RGD adhesion sequence (Figure 5C). Together, this hybrid CLP-NorHA system with tunable adhesion motifs is a versatile system to fabricate model microenvironments to study cancer growth and invasive spreading.

4. CONCLUSION

Hybrid natural-synthetic systems show immense promise for recreating tissue microenvironments, where orthogonal bioconjugation handles allow the mixing of protein, polysaccharide, and synthetic motifs. We successfully created a recombinant collagen-like protein−hyaluronic acid hydrogel with tunable peptide binding motifs. The resulting hybrid gel has strain stiffening properties that provide collagen-like structural motifs with hyaluronan networks and the ability to integrate short peptides to control cell−matrix engagement. This material is biocompatible and was demonstrated to promote cell attachment, growth, and spreading of metastatic breast cancer cells. The modular nature of this hydrogel system will allow virtually any biomolecule to be integrated toward

https://doi.org/10.1021/acsabm.2c00186
ACS Appl. Bio Mater. XXXX, XXX, XXX−XXX

more accurate models of the complex matrix in the tumor microenvironment.

■ ASSOCIATED CONTENT

Supporting Information

The Supporting Information is available free of charge at https://pubs.acs.org/doi/10.1021/acsabm.2c00186.

SDS-PAGE, ^{1}H NMR and CD spectra, FTIR characterizing the hybrid CLP-NorHA gel, and brightfield and confocal microscopy images of cells on top and embedded (PDF)

■ AUTHOR INFORMATION

Corresponding Author

Kristopher A. Kilian − *School of Chemistry and Australian Centre for NanoMedicine, University of New South Wales, Sydney, Australia 2052;* orcid.org/0000-0002-8963-9796; Email: k.kilian@unsw.edu.au

Authors

Stephanie Nemec − *School of Materials Science & Engineering, University of New South Wales, Sydney, Australia 2052; Australian Centre for NanoMedicine, University of New South Wales, Sydney, Australia 2052*

Sylvia Ganda − *School of Chemistry and Australian Centre for NanoMedicine, University of New South Wales, Sydney, Australia 2052;* orcid.org/0000-0002-3055-7841

Karrar Al Taief − *School of Chemistry, Australian Centre for NanoMedicine, and UNSW RNA Institute, University of New South Wales, Sydney, Australia 2052*

Chantal Kopecky − *School of Chemistry and Australian Centre for NanoMedicine, University of New South Wales, Sydney, Australia 2052*

Rhiannon Kuchel − *Electron Microscope Unit, Mark Wainwright Analytical Centre, University of New South Wales, Sydney, Australia 2052*

Hélène Lebhar − *School of Biotechnology and Biomolecular Sciences, University of New South Wales, Sydney, Australia 2052*

Christopher P. Marquis − *UNSW RNA Institute and School of Biotechnology and Biomolecular Sciences, University of New South Wales, Sydney, Australia 2052;* orcid.org/0000-0003-1656-7215

Pall Thordarson − *School of Chemistry, Australian Centre for NanoMedicine, and UNSW RNA Institute, University of New South Wales, Sydney, Australia 2052;* orcid.org/0000-0002-1200-8814

Complete contact information is available at: https://pubs.acs.org/10.1021/acsabm.2c00186

Author Contributions

S.N., S.G., K.A.T., H.L., C.P.M., P.T., and K.A.K. designed the experiments. S.N., S.G., C.K., R.K. and K.A.T. performed the experiments and analyzed the data. All authors contributed to writing the manuscript and have approved the final version of the manuscript.

Funding

This work was supported through funding from the Australian Research Council Grants FT180100417 (K.A.K.) and DP190101892 (P.T.), the National Health and Medical Research Council (NHMRC) Ideas Grant APP1185021 (K.A.K.), and the National Cancer Institute of the National Institutes of Health Grant R01CA251443 (K.A.K.).

Notes

The authors declare no competing financial interest.

■ ACKNOWLEDGMENTS

The authors are grateful for the support from the Recombinant Products Facility including Eve Jary and Kate Roberts. We acknowledge use of facilities in the Structural Biology Facility and helpful discussions with Drs. Anne Rich and Kate Mitchie within the Mark Wainwright Analytical Centre (MWAC), funded in part by the Australian Research Council Linkage Infrastructure, Equipment and Facilities Grant ARC LIEF 190100165. We also acknowledge the facilities and the scientific and technical support of staff at the Katharina Gaus Light Microscopy Facility as well as the Biological Specimen Preparation Laboratory of Microscopy Australia and the Electron Microscope Unit (EMU) within MWAC at UNSW Sydney especially Sean Lim. S.N. acknowledges support from a UNSW Sydney Scientia Ph.D. Scholarship.

■ ABBREVIATIONS

CLP = collagen-like protein
NorHA = norbornene functionalized hyaluronic acid
RGD = arginine-glycine-aspartate
RDG = arginine-aspartate-glycine

■ REFERENCES

(1) Hatzfeld, M.; Weber, K. The Coiled Coil of in Vitro Assembled Keratin Filaments Is a Heterodimer of Type I and II Keratins: Use of Site-Specific Mutagenesis and Recombinant Protein Expression. *J. Cell Biol.* **1990**, *110* (4), 1199−1210.

(2) Kobatake, E.; Takahashi, R.; Mie, M. Construction of a BFGF-Tethered Extracellular Matrix Using a Coiled-Coil Helical Interaction. *Bioconjugate Chem.* **2011**, *22* (10), 2038−2042.

(3) Shoseyov, O.; Posen, Y.; Grynspan, F. Human Recombinant Type I Collagen Produced in Plants. *Tissue Eng. Part A* **2013**, *19* (13−14), 1527−1533.

(4) Werkmeister, J. A.; Ramshaw, J. A. M. Recombinant Protein Scaffolds for Tissue Engineering. *Biomed. Mater.* **2012**, *7* (1), No. 012002.

(5) Aisenbrey, E. A.; Murphy, W. L. Synthetic Alternatives to Matrigel. *Nat. Rev. Mater.* **2020**, *5* (7), 539−551.

(6) Lutolf, M. P.; Hubbell, J. A. Synthetic Biomaterials as Instructive Extracellular Microenvironments for Morphogenesis in Tissue Engineering. *Nat. Biotechnol.* **2005**, *23*, 47−55.

(7) Oskarsson, T. Extracellular Matrix Components in Breast Cancer Progression and Metastasis. *Breast* **2013**, *22* (S2), S66−S72.

(8) Yang, C.; Hillas, P. J.; Báez, J. A.; Nokelainen, M.; Balan, J.; Tang, J.; Spiro, R.; Polarek, J. W. The Application of Recombinant Human Collagen in Tissue Engineering. *BioDrugs* **2004**, *18* (2), 103−119.

(9) Ye, S.; Boeter, J. W. B.; Mihajlovic, M.; Steenbeek, F. G.; Wolferen, M. E.; Oosterhoff, L. A.; Marsee, A.; Caiazzo, M.; Laan, L. J. W.; Penning, L. C.; Vermonden, T.; Spee, B.; Schneeberger, K. A Chemically Defined Hydrogel for Human Liver Organoid Culture. *Adv. Funct. Mater.* **2020**, *30* (48), 2000893.

(10) Zhu, D.; Wang, H.; Trinh, P.; Heilshorn, S. C.; Yang, F. Elastin-like Protein-Hyaluronic Acid (ELP-HA) Hydrogels with Decoupled Mechanical and Biochemical Cues for Cartilage Regeneration. *Biomaterials* **2017**, *127*, 132−140.

(11) LeSavage, B. L.; Suhar, N. A.; Madl, C. M.; Heilshorn, S. C. Production of Elastin-like Protein Hydrogels for Encapsulation and Immunostaining of Cells in 3D. *J. Vis. Exp.* **2018**, 57739.

(12) Peng, Y. Y.; Yoshizumi, A.; Danon, S. J.; Glattauer, V.; Prokopenko, O.; Mirochnitchenko, O.; Yu, Z.; Inouye, M.;

Werkmeister, J. A.; Brodsky, B.; Ramshaw, J. A. M. A Streptococcus Pyogenes Derived Collagen-like Protein as a Non-Cytotoxic and Non-Immunogenic Cross-Linkable Biomaterial. *Biomaterials* **2010**, *31* (10), 2755−2761.
(13) Qiu, Y.; Zhai, C.; Chen, L.; Liu, X.; Yeo, J. Current Insights on the Diverse Structures and Functions in Bacterial Collagen-like Proteins. *ACS Biomater. Sci. Eng.* **2021**, DOI: 10.1021/acsbiomaterials.1c00018.
(14) Cosgriff-Hernandez, E.; Hahn, M. S.; Russell, B.; Wilems, T.; Munoz-Pinto, D.; Browning, M. B.; Rivera, J.; Höök, M. Bioactive Hydrogels Based on Designer Collagens. *Acta Biomater.* **2010**, *6* (10), 3969−3977.
(15) Parmar, P. A.; Chow, L. W.; St-Pierre, J.-P.; Horejs, C.-M.; Peng, Y. Y.; Werkmeister, J. A.; Ramshaw, J. A. M.; Stevens, M. M. Collagen-Mimetic Peptide-Modifiable Hydrogels for Articular Cartilage Regeneration. *Biomaterials* **2015**, *54*, 213−225.
(16) Parmar, P. A.; Skaalure, S. C.; Chow, L. W.; St-Pierre, J.-P.; Stoichevska, V.; Peng, Y. Y.; Werkmeister, J. A.; Ramshaw, J. A. M.; Stevens, M. M. Temporally Degradable Collagen−Mimetic Hydrogels Tuned to Chondrogenesis of Human Mesenchymal Stem Cells. *Biomaterials* **2016**, *99*, 56−71.
(17) Tolg, C.; Telmer, P.; Turley, E. Specific Sizes of Hyaluronan Oligosaccharides Stimulate Fibroblast Migration and Excisional Wound Repair. *PLoS One* **2014**, *9* (2), e88479.
(18) Burdick, J. A.; Prestwich, G. D. Hyaluronic Acid Hydrogels for Biomedical Applications. *Adv. Mater.* **2011**, *23* (12), H41−56.
(19) Khunmanee, S.; Jeong, Y.; Park, H. Crosslinking Method of Hyaluronic-Based Hydrogel for Biomedical Applications. *J. Tissue Eng.* **2017**, *8*, No. 204173141772646.
(20) Gramlich, W. M.; Kim, I. L.; Burdick, J. A. Synthesis and Orthogonal Photopatterning of Hyaluronic Acid Hydrogels with Thiol-Norbornene Chemistry. *Biomaterials* **2013**, *34* (38), 9803−9811.
(21) Weiss, M. S.; Bernabé, B. P.; Shikanov, A.; Bluver, D. A.; Mui, M. D.; Shin, S.; Broadbelt, L. J.; Shea, L. D. The Impact of Adhesion Peptides within Hydrogels on the Phenotype and Signaling of Normal and Cancerous Mammary Epithelial Cells. *Biomaterials* **2012**, *33* (13), 3548−3559.
(22) Peng, Y. Y.; Stoichevska, V.; Schacht, K.; Werkmeister, J. A.; Ramshaw, J. A. M. Engineering Multiple Biological Functional Motifs into a Blank Collagen-like Protein Template from *Streptococcus Pyogenes*. *J. Biomed. Mater. Res. Part A* **2014**, *102* (7), 2189−2196.
(23) Trujillo, S.; Vega, S. L.; Song, K. H.; San Félix, A.; Dalby, M. J.; Burdick, J. A.; Salmeron-Sanchez, M. Engineered Full-Length Fibronectin−Hyaluronic Acid Hydrogels for Stem Cell Engineering. *Adv. Healthc. Mater.* **2020**, *9* (21), 2000989.
(24) Broedersz, C. P.; Kasza, K. E.; Jawerth, L. M.; Münster, S.; Weitz, D. A.; MacKintosh, F. C. Measurement of Nonlinear Rheology of Cross-Linked Biopolymer Gels. *Soft Matter.* **2010**, *6*, 4120−4127.
(25) Parmar, P. A.; Skaalure, S. C.; Chow, L. W.; St-Pierre, J. P.; Stoichevska, V.; Peng, Y. Y.; Werkmeister, J. A.; Ramshaw, J. A. M.; Stevens, M. M. Temporally Degradable Collagen-Mimetic Hydrogels Tuned to Chondrogenesis of Human Mesenchymal Stem Cells. *Biomaterials* **2016**, *99*, 56−71.
(26) Motte, S.; Kaufman, L. J. Strain Stiffening in Collagen i Networks. *Biopolymers* **2013**, *99* (1), 35−46.
(27) Piechocka, I. K.; Bacabac, R. G.; Potters, M.; Mackintosh, F. C.; Koenderink, G. H. Structural Hierarchy Governs Fibrin Gel Mechanics. *Biophys. J.* **2010**, *98* (10), 2281−2289.
(28) Vinci, M.; Box, C.; Zimmermann, M.; Eccles, S. A. Tumor Spheroid-Based Migration Assays for Evaluation of Therapeutic Agents. *Methods Mol. Biol.* **2013**, *986*, 253−266.

https://doi.org/10.1021/acsabm.2c00186
ACS Appl. Bio Mater. XXXX, XXX, XXX−XXX